

Dynamics of Multi-Component Flows: Diffusive Interface Methods With Energetic Variational Approaches[☆]

J Brannick, A Kirshtein, and C Liu, Penn State University, University Park, PA, USA

© 2016 Elsevier Inc. All rights reserved.

Introduction	1
1 Two Fluids Mixture	2
2 Boundary Conditions	4
3 Mixture of Three Fluids	5
References	6

Introduction

Complex fluids are those with internal microstructures whose evolution affects the macroscopic dynamics of the material, especially the rheology. Examples include polymer solutions and melts, liquid crystals, gels, suspensions, emulsions and micellar solutions (Larson, 1999). Such materials often have great practical utility since the microstructure can be manipulated via processing of the flow in order to produce useful mechanical, optical or thermal properties. An important way of utilizing complex fluids is through composites. By blending two immiscible components together, one may derive novel or enhanced properties from the composite, and this is often a more economical route to new materials than synthesis. Moreover, the properties of composites may be tuned to suit a particular application by varying the composition, concentration and, most importantly, the phase morphology. Perhaps the most important of such composites are polymer blends (Utracki and Favis, 1989). Under optimal processing conditions, the dispersed phase is stretched into a fibrillar morphology. Upon solidification, the long fibers act as in situ reinforcement and impart great strength to the composite. The effect is particularly strong if the fibrillar phase is a liquid-crystalline polymer (National Materials Advisory Board, National Research Council, 1990). Another example is polymer-dispersed liquid crystals, with liquid crystal droplets embedded in a polymer matrix, which have shown great potential in electro-optical applications (West, 1990).

From a fundamental viewpoint, such composites are extremely interesting. They feature dynamic coupling of three disparate length scales: molecular or supramolecular conformation inside each component, mesoscopic interfacial morphology and macroscopic hydrodynamics. The complexity of such materials has for the most part prohibited theoretical and numerical analysis. The main difficulty is the moving and deforming interface between the two components. Traditional fluid dynamics treats these as sharp interfaces on which matching conditions must be imposed.

There are various approaches that have been developed to model complex flows. The boundary integral and boundary element methods use a mesh with grid points that lie on the interfaces and deforms according to the flow on both sides of the boundary (Cristini *et al.*, 1998; Toose *et al.*, 1995; Kelly *et al.*, 1983). These include works on finite-element methods (Hu *et al.*, 2001; Ambravaneswaran *et al.*, 2002; Hooper *et al.*, 2001a,b; Kim and Han, 2001) and finite-difference methods (Ramaswamy and Leal, 1999b,a). Two drawbacks of these approaches are that keeping track of the moving mesh can entail a large computational overhead and large displacement of internal domains can result in mesh entanglement as happens, say, when one drop overtakes another. Typically, a remeshing scheme is activated, introducing geometric error into the discrete approximation (interpolation error) as well as additional computational cost. Most importantly, the moving-mesh methods cannot handle singular morphological changes such as breakup, coalescence, and reconnection; the sharp interface formulation breaks down in such cases. Thus, these methods have so far been limited mostly to single drops undergoing relatively mild deformations.

As an alternative, fixed-grid methods that regularize the interface have been highly successful in treating deforming interfaces. These include the volume-of-fluid (VOF) method (Li and Renardy, 2000a), the front-tracking method (Unverdi and Tryggvason, 1992) and the level-set method (Sethian and Smereka, 2003; Zheng and Zhang, 2000; Chang *et al.*, 1996). Instead of formulating the flow of two domains separated by an interface, these methods represent the interfacial tension as a body force or bulk stress spread over a narrow region covering the interface. Then a single set of governing equations can be written over the entire domain which can be solved on a fixed grid in a purely Eulerian framework, as in Li and Renardy (2000b); the overview paper (Sethian and Smereka, 2003) gives an insightful comparison of such approaches.

[☆]Change History: June 2015. C. Liu, J. Brannick and A. Kirshtein made minor typo, formatting and other pre-submission corrections. Changed links to figures 1–2 in the text, and changed the energy dissipation and boundary conditions in section 2 (Boundary conditions) to a more conventional form.

Here we focus on the diffusive interface method, which uses a phase field to smoothen the transition between two phases (Liu and Shen, 2003). The approach can be viewed as a physically motivated level-set method. Instead of choosing an artificial smoothing function for the interface, which affects the results in non-trivial ways if the radius of interfacial curvature approaches that of the interfacial thickness (Lowengrub and Truskinovsky, 1998), the diffuse interface model describes the interface by a mixing energy. This idea can be traced to van der Waals (1979), (first published in 1892), it has been widely used and successfully incorporated to numerous practical applications, including models of phase transitions (Hohenberg and Halperin, 1977; Caginalp, 1986; Wheeler *et al.*, 1992), contact line dynamics in complex fluids (Liu and Shen, 2003; Qian *et al.*, 2003, 2006; Brannick *et al.*, 2015; Yue *et al.*, 2004), cell motility (Aronson, 2014), and many other problems in science and engineering. Thus, the structure of the interface is determined by molecular forces; in particular, the tendencies for mixing and demixing are balanced through the non-local mixing energy. Moreover, when the capillary width approaches zero, the diffuse interface model becomes identical to a sharp interface level-set formulation. The method also reduces properly to the classical sharp interface model.

To build a diffusive interface model of complex fluid flow, one can use concentration, mass fraction or volume fraction as a phase field and builds a model based on conservation of mass, conservation of momentum and other physical assumptions (Lowengrub and Truskinovsky, 1998; Boyer, 2002; Abels *et al.*, 2012). Another approach is to write the second law of thermodynamics in terms of total energy and energy dissipation, and use variational techniques to obtain a mathematical model (Qian *et al.*, 2006; Hyon *et al.*, 2010), which under some natural assumptions leads to coupled systems of time dependent and nonlinear partial differential equations (PDEs) that can be simulated numerically. Typically, the system of PDEs consists of the Navier-Stokes equations coupled to either the Allen–Cahn system (NS-AC), or the Cahn–Hilliard (NS-CH) system.

There are three main challenges for solving these systems numerically: the nonlinearity in the mathematical model, the presence of the interface, which usually is thin in phase transition applications, and the different time scales of each of the stages in the evolution of the concentration. Overall, an efficient numerical resolution of the problem requires proper relation of numerical scales, that is, the (spatial) mesh size h and the (time) step size Δt have to properly relate to the interaction length ε . Numerous discretizations and solvers have been developed to handle these difficulties for two phase systems, which have since led to promising results for various applications.

A unified approach on how to design simple, efficient and energy stable time discretization schemes for the NS-AC and NS-CH systems (for matching or non-matching density) is found by Shen (2011). Recent works on numerically solving the three phase NS-CH system are found in Kim *et al.* (2004b); Kim *et al.* (2004a); Lee *et al.* (2012); Shin *et al.* (2013); Gao and Wang (2012, 2014); Boyer *et al.* (2010); Tierra and Guillen-Gonzalez (2014); Guillen-Gonzalez and Tierra (2014); Boyer *et al.* (2009); and Brannick *et al.* (2015) considers the three phase NS-AC system.

1 Two Fluids Mixture

Let us consider phase field satisfying

$$\varphi(\mathbf{x}) = \begin{cases} 1, & \text{in substance 1,} \\ -1, & \text{in substance 2,} \end{cases}$$

which takes values in $(-1, 1)$ on the diffusive interface. φ may not be an obvious physical quantity (like concentration or volume fraction), but just a labeling function representing the smooth transition between phases.

Following Cahn and Hilliard (1958), we introduce the mixing energy as a functional of φ

$$\mathcal{W}(\varphi) = \int \frac{1}{2} |\nabla \varphi|^2 + \frac{1}{\varepsilon^2} F(\varphi) dx \quad [1]$$

Where F is a so-called double-well potential (e.g., $F(\varphi) = \frac{1}{4}(\varphi^2 - 1)^2$), ε is a parameter responsible for the ‘width’ of the interface. The gradient term in this energy is diffusive (‘philic,’ represents weakly non-local interactions between the components that prefers complete mixing), while the second term is Ginzburg-Landau potential (repulsion potential, ‘phobic,’ prefers total separation of the phases). The competition between the two effects defines the profile of φ across the interface (see Figure 1 for minimizer of \mathcal{W} in one space dimension).

Now we combine the mixing energy with hydrodynamic kinetic energy, and write the energy law

$$\frac{d}{dt} \left[\int \frac{\rho(\varphi) |\mathbf{u}|^2}{2} dx + \sigma \frac{3\varepsilon}{2\sqrt{2}} \mathcal{W}(\varphi) \right] = -2\mathcal{D} \quad [2]$$

Here σ is the interface surface tension constant (note that $\mathcal{W}\left(\tanh\left(\frac{x}{\sqrt{2\varepsilon}}\right)\right) = \frac{2\sqrt{2}}{3\varepsilon}$, $x \in \mathbb{R}$). Velocity \mathbf{u} is taken to be incompressible background velocity (e.g., volume averaged Abels *et al.* (2012)), not the velocity of either of phases. According to

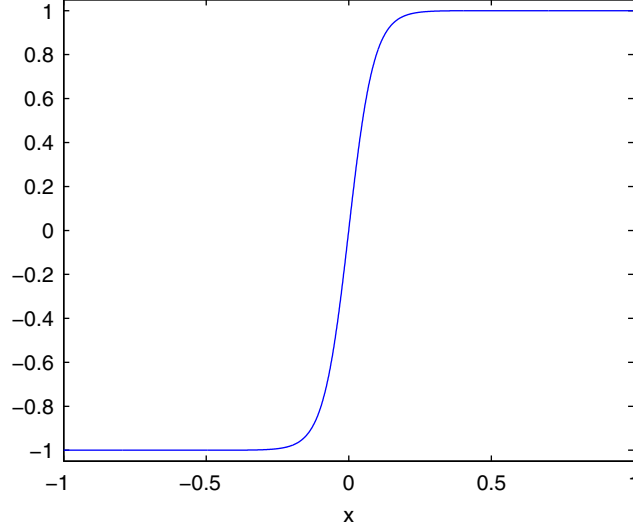


Figure 1 Minimizer of energy (1), $\varphi(x) = \tanh\left(\frac{x}{\sqrt{2\varepsilon}}\right)$, for $\varepsilon = 1/16$ – interface width parameter.

Onsager (1931b,a) the energy dissipation D (the quantity $2D$ is also called entropy production) should be proportional to some ‘rate’ raised to a second power. Let us write it as a sum of viscous dissipation

$$\frac{1}{4} \int \eta(\varphi) |\nabla \mathbf{u} + \nabla \mathbf{u}^T|^2 dx$$

and dissipation on the interface

$$\frac{1}{2} \int \varphi^2 \langle M^{-1}(\varphi)(\mathbf{V} - \mathbf{u}), (\mathbf{V} - \mathbf{u}) \rangle dx$$

Here \mathbf{V} is effective velocity of the phase field

$$\varphi_t + \nabla \cdot (\mathbf{V}\varphi) = 0 \quad [3]$$

Note that this ensures conservation of the phase field φ . Then we combine the variational Principle of Least Action (LAP) (Arnol’d, 1989) and Maximum Dissipation Principle (MDP) (Hyon *et al.*, 2010). To apply LAP, we have to consider to separate independent flow maps related to \mathbf{u} and \mathbf{V} . Writing the action functional

$$\mathcal{F} = \int \frac{\rho(\varphi)|\mathbf{u}|^2}{2} dx - \sigma \frac{3\varepsilon}{2\sqrt{2}} \mathcal{W}(\varphi)$$

and applying the variation (in Lagrangian coordinates, with $\nabla \cdot \mathbf{u} = 0$ constraint in the first case) we get

$$\begin{cases} \frac{\delta \mathcal{F}}{\delta \mathbf{x}_\mathbf{u}} = -\rho(\varphi) D_t \mathbf{u} - \sigma \frac{3\varepsilon}{2\sqrt{2}} \nabla \cdot (\nabla \varphi \otimes \nabla \varphi) - \nabla p, \\ \frac{\delta \mathcal{F}}{\delta \mathbf{x}_\varphi} = -\varphi \nabla \mu, \\ \mu = \sigma \frac{3\varepsilon}{2\sqrt{2}} \left(-\Delta \varphi + \frac{1}{\varepsilon^2} (\varphi^2 - 1) \varphi \right) + \rho'(\varphi) \frac{|\mathbf{u}|^2}{2}. \end{cases}$$

Here $D_t \varphi = \varphi_t + \mathbf{u} \cdot \nabla \varphi$ is material derivative. Because of scale separation, for each variation in MDP we using only corresponding part of dissipation: viscous dissipation for variation with respect to \mathbf{u} and interface dissipation for variation with respect to \mathbf{V} . The result we get is

$$\begin{cases} \rho(\varphi) D_t \mathbf{u} + \sigma \frac{3\varepsilon}{2\sqrt{2}} \nabla \cdot (\nabla \varphi \otimes \nabla \varphi) + \nabla p = \nabla \cdot (\eta(\varphi) (\nabla \mathbf{u} + \nabla \mathbf{u}^T)) \\ -\varphi \nabla \mu = \varphi^2 M(\varphi) (\mathbf{V} - \mathbf{u}). \end{cases}$$

Combining this with [3] we get the Navier–Stokes/Cahn–Hilliard system:

$$\begin{cases} D_t \varphi = \nabla \cdot (M(\varphi) \nabla \zeta), \\ \rho(\varphi) D_t \mathbf{u} = -\nabla p + \nabla \cdot (\eta(\varphi) (\nabla \mathbf{u} + \nabla \mathbf{u}^T)) - \sigma \frac{3\varepsilon}{2\sqrt{2}} \nabla \cdot (\nabla \varphi \otimes \nabla \varphi), \\ \nabla \cdot \mathbf{u} = 0, \\ \mu = \sigma \frac{3\varepsilon}{2\sqrt{2}} \left(-\Delta \varphi + \frac{1}{\varepsilon^2} (\varphi^2 - 1) \varphi \right) + \rho'(\varphi) \frac{|\mathbf{u}|^2}{2}. \end{cases} \quad [4]$$

Remark 1: The sharp interface model assumes that the phases are subject to pure convection. Cahn–Hilliard equation is perturbation from that. Another way to perturb convection is Allen–Cahn equation, which is a gradient flow in φ :

$$D_t \varphi = -m(\varphi) \mu$$

In the energy law this model would correspond to the following term related to dissipation on the interface:

$$\frac{1}{2} \int \frac{1}{m(\varphi)} |D_t \varphi|^2 dx$$

It is important to notice, that (unlike Cahn–Hilliard) this model does not have conservation of φ . But it does have other advantages (e.g., maximum principle, see [Onsager, 1931a,b](#)).

Remark 2: Consider the Oldroyd model for the incompressible viscoelastic fluid:

$$\begin{cases} F_t + \mathbf{v} \cdot \nabla F = \nabla \mathbf{v} F, \\ \mathbf{v}_t + \mathbf{v} \cdot \nabla \mathbf{v} + \nabla p = \eta \Delta \mathbf{v} + \nabla \cdot (FF^T) \\ \nabla \cdot \mathbf{v} = 0. \end{cases}$$

Under assumption that $\det F_0 = 1$, we can claim that $F = \nabla \times \varphi$ (here φ is a matrix), and rewrite the system as

$$\begin{cases} \varphi_t + \mathbf{v} \cdot \nabla \varphi = 0, \\ \mathbf{v}_t + \mathbf{v} \cdot \nabla \mathbf{v} + \nabla p = \eta \Delta \mathbf{v} + \nabla \cdot (\nabla \varphi \otimes \nabla \varphi), \\ \nabla \cdot \mathbf{v} = 0, \end{cases}$$

which is similar to the system [4] with no interface diffusion ($M(\varphi) = 0$) [for more details see [Lin et al., 2005](#)].

Remark 3: It is of certain interest to analyze sharp interface limit with $\varepsilon \rightarrow 0$. See [Abels et al. \(2012\)](#) for an example of formal asymptotic analysis using inner and outer expansions.

2 Boundary Conditions

If we consider the energy law [2] on a bounded domain Ω , then integration by parts in both LAP and MDP will require boundary conditions

$$\begin{cases} \langle \nabla \varphi, \mathbf{n} \rangle = 0, \\ \langle M(\varphi) \nabla \zeta, \mathbf{n} \rangle = 0, \quad \mathbf{x} \in \partial \Omega, \quad t > 0. \\ \mathbf{u} = 0. \end{cases}$$

However, [Qian et al. \(2006\)](#) have shown that the model with energy dissipation at the solid boundary surface better matches molecular dynamics experiments, and avoids discrepancy of the contact line dynamics. More precisely, standard boundary conditions do not allow contact line to move along the boundary, while molecular dynamics experiments show, that near complete slip occurs in vicinity of contact line near the boundary.

Hence, we consider the following expression for energy dissipation (including bulk terms already mentioned above):

$$\mathcal{D} = \frac{1}{2} \int_{\Omega} \left(\frac{1}{2} \eta(\varphi) |\nabla \mathbf{u} + \nabla \mathbf{u}^T|^2 + \varphi^2 \langle M^{-1}(\varphi) (\mathbf{V} - \mathbf{u}), (\mathbf{V} - \mathbf{u}) \rangle \right) dx + \frac{1}{2} \int_{\partial \Omega} \left(\beta |\mathbf{u}_{\tau}^{slip}|^2 + \frac{3\varepsilon}{2\sqrt{2}} \frac{\sigma}{\gamma} |\varphi_t + \mathbf{u}_{\tau} \cdot \nabla_{\tau} \varphi|^2 \right) dS_x,$$

where \mathbf{u}^{slip} is velocity relative to the boundary (if boundary is not moving, $\mathbf{u}^{slip} = \mathbf{u}$), and subscript τ denotes components tangential to the boundary (e.g., $\mathbf{u}_{\tau} = \mathbf{u} - (\mathbf{u} \cdot \mathbf{n}) \mathbf{n}$). The force balance after combining LAP and MDP results into the dynamic boundary

conditions on φ and generalized Navier boundary conditions on \mathbf{u} :

$$\begin{cases} \varphi_t + \mathbf{u}_\tau \cdot \nabla_\tau \varphi + \gamma \partial_{\mathbf{n}} \varphi = 0, & \langle M(\varphi) \nabla \zeta, \mathbf{n} \rangle = 0, \\ \beta(\mathbf{u}_\tau^{\text{slip}}) + \eta(\varphi) \partial_{\mathbf{n}}(\mathbf{u}_\tau) - \sigma \frac{3\varepsilon}{2\sqrt{2}} \partial_{\mathbf{n}} \varphi \nabla_\tau \varphi = 0, \\ \mathbf{u} \cdot \mathbf{n} = 0, & \mathbf{x} \in \partial\Omega, \quad t > 0. \end{cases}$$

Remark 4: In generalized Navier boundary conditions the term $\sigma \frac{3\varepsilon}{2\sqrt{2}} \partial_{\mathbf{n}} \varphi \nabla_\tau \varphi$ is the so-called uncompensated Young stress. See [Qian et al. \(2006\)](#) for expression in terms of contact angle and physical interpretation.

Remark 5: The case above considers the equilibrium contact angle ([De Gennes et al., 2004](#); [Rowlinson and Widom, 2002](#)) to be $\pi/2$. For more general contact angle θ_c [Qian et al. \(2006\)](#) suggest boundary condition

$$\begin{cases} \varphi_t + \mathbf{u}_\tau \cdot \nabla_\tau \varphi + \gamma \partial_{\mathbf{n}} \varphi = 0, & \langle M(\varphi) \nabla \zeta, \mathbf{n} \rangle = 0, \\ \beta(\mathbf{u}_\tau^{\text{slip}}) + \eta(\varphi) \partial_{\mathbf{n}}(\mathbf{u}_\tau) - \sigma \frac{3\varepsilon}{2\sqrt{2}} L(\varphi) \nabla_\tau \varphi = 0, \\ \mathbf{u} \cdot \mathbf{n} = 0, & \mathbf{x} \in \partial\Omega, \quad t > 0, \\ L(\varphi) = \partial_{\mathbf{n}} \varphi + \partial \gamma_{fs}(\varphi) / \partial \varphi, \end{cases}$$

where $\gamma_{fs} = \frac{c_b}{2} \cos \theta_c \sin(\pi\varphi/2)$ is an additional interfacial free energy density. The total energy considered in this case should be

$$\int_{\Omega} \frac{\rho(\varphi) |\mathbf{u}|^2}{2} d\mathbf{x} + \sigma \frac{3\varepsilon}{2\sqrt{2}} \left(\mathcal{W}(\varphi) + \int_{\partial\Omega} \gamma_{fs} dS_x \right)$$

3 Mixture of Three Fluids

Here we discuss several results for mixtures of more than two phases.

[Kim and Lowengrub \(2005\)](#) developed a thermodynamically consistent model for three-phase flow, where they use concentrations as a phase variables. However, they use mass-averaged velocity for the background flow, which is quasi-incompressible (see [Lowengrub and Truskinovsky, 1998](#); [Abels et al., 2012](#)).

[Boyer and Lapuerta \(2006\)](#); [Boyer et al. \(2010\)](#) build a model for three phase flow using LAP with Lagrange multiplier to find a chemical potentials μ for each phase. They use volume averaged velocity to ensure incompressibility condition, which is preferable from numerical prospective. The phase part of the model they build is

$$\begin{cases} c_t = M_1 \Delta \zeta_c, & d_t = M_2 \Delta \zeta_d, \\ \zeta_c = -\frac{3}{4} \varepsilon \nabla \cdot (\Sigma_1 \nabla c) + \frac{12}{\varepsilon} \partial_1 F(\mathbf{c}) + \beta, \\ \zeta_d = -\frac{3}{4} \varepsilon \nabla \cdot (\Sigma_2 \nabla d) + \frac{12}{\varepsilon} \partial_2 F(\mathbf{c}) + \beta, \\ \beta = -\Sigma_0 \left(\frac{1}{\Sigma_1} \partial_1 F(\mathbf{c}) + \frac{1}{\Sigma_2} \partial_2 F(\mathbf{c}) + \frac{1}{\Sigma_3} \partial_3 F(\mathbf{c}) \right) \\ \mathbf{c} = \langle c, d, 1 - c - d \rangle, \\ \Sigma_0 = (\Sigma_1^{-1} + \Sigma_2^{-1} + \Sigma_3^{-1})^{-1}, \\ M_1 \Sigma_1 = M_2 \Sigma_2 = M_3 \Sigma_3 = M_0. \end{cases}$$

[Boyer et al.](#) show that Lagrange multiplier, mobility constraint and some additional requirements on repulsion potential F are necessary to ensure energetic and dynamic consistency with a two-phase model in any combination ($c \equiv 0, d \equiv 0, c + d \equiv 1$). Among other requirements, they ensure the third phase will not artificially appear in the region where only two phases are present. Authors confirm their analysis with numerical experiment (for example of implementation in 3D see in [Figure 2\(b\)](#)).

The Allen–Cahn/Navier–Stokes model by [Brannick et al. \(2015\)](#) was built using LAP and MDP for the case of constant (negligibly different) densities. Here authors use two labeling functions as a phase variables. The resulting system is

$$\begin{cases} \rho(\mathbf{u}_t + \mathbf{u} \cdot \nabla \mathbf{u}) + \nabla p = \nabla \cdot (\lambda \sigma^e + 2\mu \sigma^v) \\ \phi_t + \mathbf{u} \cdot \nabla \phi = -M_1 \frac{\delta E}{\delta \phi}, \\ \psi_t + \mathbf{u} \cdot \nabla \psi = -M_2 \frac{\delta E}{\delta \psi}, \\ \nabla \cdot \mathbf{u} = 0, \end{cases} \quad [5]$$

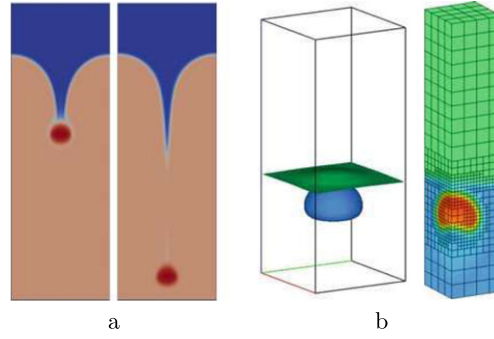


Figure 2 (a) A solid particle with a slippery surface falling in a binary fluid (Brannick *et al.*, 2015); (b) An example of adaptive local refinement in 3D used in Boyer *et al.* (2010).

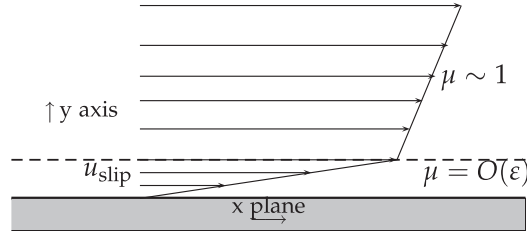


Figure 3 A schematic illustration of fluid slip modeled by a fast variation of tangential velocity across a thin layer (diffuse interface) with a small viscosity μ .

where

$$\begin{aligned}\frac{\delta E}{\delta \phi} &= \gamma_1 \left\{ -\varepsilon_1 \nabla \cdot \left[\left(\frac{\psi - 1}{2} \right)^2 \nabla \phi \right] + \frac{1}{\varepsilon_1} \left(\frac{\psi - 1}{2} \right)^2 (\phi^2 - 1) \phi \right\} \\ \frac{\delta E}{\delta \psi} &= \gamma_2 \left\{ -\varepsilon_2 \Delta \psi + \frac{1}{\varepsilon_2} (\psi^2 - 1) \psi \right\} + \gamma_1 \frac{\psi - 1}{2} \left\{ \frac{\varepsilon_1}{2} |\nabla \phi|^2 + \frac{1}{4\varepsilon_1} (\phi^2 - 1)^2 \right\}, \\ \sigma^e &= -\gamma_1 \varepsilon_1 \left(\frac{\psi - 1}{2} \right)^2 \nabla \phi \otimes \nabla \phi - \gamma_2 \varepsilon_2 \nabla \psi \otimes \nabla \psi, \quad \sigma^v = \frac{1}{2} [\nabla \mathbf{u} + (\nabla \mathbf{u})^T].\end{aligned}$$

The authors analyze the model numerically in different configurations (Boussinesq approximation was used to incorporate gravity). Authors show analytically that the slip effect on the boundary of a solid may be introduced by a thin layer of nearly inviscid fluid (see [Figure 3](#)), and qualitatively confirm this result with numerical experiment (see [Figure 2\(a\)](#)).

References

- Abels, H., Garcke, H., Grun, G., 2012. Thermodynamically consistent, frame indifferent diffuse interface models for incompressible two-phase flows with different densities. *Mathematical Models and Methods in Applied Sciences* 22 (03), 1–39.
- Ambravaneswaran, B., Wilkes, E.D., Basaran, O.A., 2002. Drop formation from a capillary tube: Comparison of one-dimensional and two-dimensional analyses and occurrence of satellite drops. *Physics of Fluids* (1994-present) 14 (8), 2606–2621.
- Arnol'd, V.I., 1989. *Mathematical methods of classical mechanics*, vol. 60. Springer.
- Aronson, I., 2014. Modeling crawling cell movement on soft engineered substrates. *Soft Matter* 10 (9), 1365–1373.
- Boyer, F., 2002. A theoretical and numerical model for the study of incompressible mixture flows. *Computers & Fluids* 31 (1), 41–68.
- Boyer, F., Lapuerta, C., 2006. Study of a three component Cahn–Hilliard flow model. *ESAIM: Mathematical Modelling and Numerical Analysis* 40 (04), 653–687.
- Boyer, F., Lapuerta, C., Minjeaud, S., Piar, B., 2009. A local adaptive refinement method with multigrid preconditioning illustrated by multiphase flows simulations. *ESAIM: Proceedings*. EDP Sciences. pp. 15–53.
- Boyer, F., Lapuerta, C., Minjeaud, S., Piar, B., Quintard, M., 2010. Cahn–Hilliard/Navier–Stokes model for the simulation of three-phase flows. *Transport in Porous Media* 82 (3), 463–483.
- Brannick, J., Liu, C., Qian, T., Sun, H., 2015. Diffuse Interface Methods for Multiple Phase Materials: An Energetic Variational Approach. *Numerical Mathematics: Theory, Methods and Applications* 8 (02), 220–236.
- Caginalp, G., 1986. An analysis of a phase field model of a free boundary. *Archive for Rational Mechanics and Analysis* 92 (3), 205–245.
- Cahn, J.W., Hilliard, J.E., 1958. Free energy of a nonuniform system. I. Interfacial free energy. *The Journal of Chemical Physics* 28 (2), 258–267.

- Chang, Y.-C., Hou, T., Merriman, B., Osher, S., 1996. A level set formulation of Eulerian interface capturing methods for incompressible fluid flows. *Journal of Computational Physics* 124 (2), 449–464.
- Cristini, V., Blawdziewicz, J., Loewenberg, M., 1998. Drop breakup in three-dimensional viscous flows. *Physics of Fluids* (1994-present) 10 (8), 1781–1783.
- De Gennes, P.-G., Brochard-Wyart, F., Quere, D., 2004. *Capillarity and Wetting Phenomena: Drops, Bubbles, Pearls, Waves*. Springer Science & Business Media.
- Gao, M., Wang, X.-P., 2012. A gradient stable scheme for a phase field model for the moving contact line problem. *Journal of Computational Physics* 231 (4), 1372–1386.
- Gao, M., Wang, X.-P., 2014. An efficient scheme for a phase field model for the moving contact line problem with variable density and viscosity. *Journal of Computational Physics* 272, 704–718.
- Guillen-Gonzalez, F., Tierra, G., 2014. Splitting schemes for a Navier–Stokes–Cahn–Hilliard model for two fluids with different densities. *JCM* 32 (6), 643–664.
- Hohenberg, P.C., Halperin, B.I., 1977. Theory of dynamic critical phenomena. *Reviews of Modern Physics* 49 (3), 435.
- Hooper, R., Toose, M., Macosko, C.W., Derby, J.J., 2001a. A comparison of boundary element and finite element methods for modeling axisymmetric polymeric drop deformation. *International Journal for Numerical Methods in Fluids* 37 (7), 837–864.
- Hooper, R.W., de Almeida, V.F., Macosko, C.W., Derby, J.J., 2001b. Transient polymeric drop extension and retraction in uniaxial extensional flows. *Journal of Non-Newtonian Fluid Mechanics* 98 (2), 141–168.
- Hu, H.H., Patankar, N.A., Zhu, M., 2001. Direct numerical simulations of fluid-solid systems using the arbitrary Lagrangian-Eulerian technique. *Journal of Computational Physics* 169 (2), 427–462.
- Hyon, Y., Kwak, D.Y., Liu, C., 2010. Energetic variational approach in complex fluids: Maximum dissipation principle. *DCDS-A* 24 (4), 1291–1304.
- Kelly, D., Gago, D.S., Zienkiewicz, O., Babuska, I., 1983. A posteriori error analysis and adaptive processes in the finite element method: Part I – Error analysis. *International Journal for Numerical Methods in Engineering* 19 (11), 1593–1619.
- Kim, J., Kang, K., Lowengrub, J., 2004a. Conservative multigrid methods for Cahn–Hilliard fluids. *Journal of Computational Physics* 193 (2), 511–543.
- Kim, J., Kang, K., Lowengrub, J., 2004b. Conservative multigrid methods for ternary Cahn–Hilliard systems. *Communications in Mathematical Sciences* 2 (1), 53–77.
- Kim, J., Lowengrub, J., 2005. Phase field modeling and simulation of three-phase flows. *Interfaces and free boundaries* 7 (4), 435.
- Kim, S.J., Han, C.D., 2001. Finite element analysis of axisymmetric creeping motion of a deformable non-Newtonian drop in the entrance region of a cylindrical tube. *Journal of Rheology* (1978-present) 45 (6), 1279–1303.
- Larson, R.G., 1999. *The Structure and Rheology of Complex Fluids*. New York: Oxford University Press.
- Lee, H.G., Choi, J.-W., Kim, J., 2012. A practically unconditionally gradient stable scheme for the N-component Cahn–Hilliard system. *Physica A: Statistical Mechanics and its Applications* 391 (4), 1009–1019.
- Li, J., Renardy, Y., 2000a. Numerical study of flows of two immiscible liquids at low Reynolds number. *SIAM Review* 42 (3), 417–439.
- Li, J., Renardy, Y.Y., 2000b. Shear-induced rupturing of a viscous drop in a Bingham liquid. *Journal of Non-Newtonian Fluid Mechanics* 95 (2), 235–251.
- Lin, F.-H., Liu, C., Zhang, P., 2005. On hydrodynamics of viscoelastic fluids. *Communications on Pure and Applied Mathematics* 58 (11), 1437–1471.
- Liu, C., Shen, J., 2003. A phase field model for the mixture of two incompressible fluids and its approximation by a Fourier-spectral method. *Physica D: Nonlinear Phenomena* 179 (3), 211–228.
- Lowengrub, J., Truskinovsky, L., 1998. Quasi-incompressible Cahn–Hilliard fluids and topological transitions. *Proceedings of the Royal Society of London. Series A: Mathematical, Physical and Engineering Sciences* 454 (1978), 2617–2654.
- National Materials Advisory Board, National Research Council, National Research Council, 1990. *Liquid Crystalline Polymers*. The National Academies Press.
- Onsager, L., 1931a. Reciprocal relations in irreversible processes. I. *Physical Review* 37 (4), 405.
- Onsager, L., 1931b. Reciprocal relations in irreversible processes. II. *Physical Review* 38 (12), 2265.
- Qian, T., Wang, X.-P., Sheng, P., 2003. Molecular scale contact line hydrodynamics of immiscible flows. *Physical Review E* 68 (1), 016306.
- Qian, T., Wang, X.-P., Sheng, P., 2006. A variational approach to moving contact line hydrodynamics. *Journal of Fluid Mechanics* 564, 333–360.
- Ramaswamy, S., Leal, L., 1999a. The deformation of a Newtonian drop in the uniaxial extensional flow of a viscoelastic liquid. *Journal of Non-Newtonian Fluid Mechanics* 88 (1), 149–172.
- Ramaswamy, S., Leal, L., 1999b. The deformation of a viscoelastic drop subjected to steady uniaxial extensional flow of a Newtonian fluid. *Journal of Non-Newtonian Fluid Mechanics* 85 (2), 127–163.
- Rowlinson, J.S., Widom, B., 2002. *Molecular Theory of Capillarity*. Mineola, N.Y.: Dover Publications.
- Sethian, J., Smereka, P., 2003. Level set methods for fluid interfaces. *Annual Review of Fluid Mechanics* 35 (1), 341–372.
- Shen, J., 2011. Modeling and numerical approximation of two-phase incompressible flows by a phase-field approach. *Multiscale Modeling and Analysis for Materials Simulation*. World Scientific. IMS, NUS, pp. 147–195.
- Shin, J., Kim, S., Lee, D., Kim, J., 2013. A parallel multigrid method of the Cahn–Hilliard equation. *Computational Materials Science* 71, 89–96.
- Tierra, G., Guillen-Gonzalez, F., 2014. Numerical methods for solving the Cahn–Hilliard equation and its applicability to related energy-based models. *Archives of Computational Methods in Engineering*. 1–21.
- Toose, E., Geurts, B., Kuerten, J., 1995. A boundary integral method for two-dimensional (non)-Newtonian drops in slow viscous flow. *Journal of Non-Newtonian Fluid Mechanics* 60 (2), 129–154.
- Unverdi, S.O., Tryggvason, G., 1992. A front-tracking method for viscous, incompressible, multi-fluid flows. *Journal of Computational Physics* 100 (1), 25–37.
- Utracki, L., Favis, B., 1989. *Polymer Alloys and Blends*, vol. 4. New York: Marcel Dekker.
- van der Waals, J., 1979. The thermodynamic theory of capillarity under the hypothesis of a continuous variation of density. *Journal of Statistical Physics* 20 (2), 200–244.
- West, J.L., 1990. *Polymer-Dispersed Liquid Crystals*. In: Weiss, R.A., Ober, C.K. (Eds.), *Liquid-Crystalline Polymers*, Chapter 32, vol. 435 of ACS Symposium Series. ACS Publications, pp. 475–495.
- Wheeler, A., Boettinger, W., McFadden, G., 1992. Phase-field model for isothermal phase transitions in binary alloys. *Physical Review A* 45 (10), 7424.
- Yue, P., Feng, J.J., Liu, C., Shen, J., 2004. A diffuse-interface method for simulating two-phase flows of complex fluids. *Journal of Fluid Mechanics* 515, 293–317.
- Zheng, L., Zhang, H., 2000. An adaptive level set method for moving-boundary problems: application to droplet spreading and solidification. *Numerical Heat Transfer: Part B: Fundamentals* 37 (4), 437–454.